



Seismic stability analysis of concrete gravity dams with penetrated cracks

Shou-yan JIANG*, Cheng-bin DU

College of Mechanics and Materials, Hohai University, Nanjing 210098, P. R. China

Abstract: The seismic stability of a cracked dam was examined in this study. Geometric nonlinearity and large deformations, as well as the contact condition at the crack site, were taken into consideration. The location of penetrated cracks was first identified using the concrete plastic-damage model based on the nonlinear finite element method (FEM). Then, the hard contact algorithm was used to simulate the crack interaction in the normal direction, and the Coloumb friction model was used to simulate the crack interaction in the tangential direction. After verification of numerical models through a case study, the seismic stability of the Koyna Dam with two types of penetrated cracks is discussed in detail with different seismic peak accelerations, and the collapse processes of the cracked dam are also presented. The results show that the stability of the dam with two types of penetrated cracks can be ensured in an earthquake with a magnitude of the original Koyna earthquake, and the cracked dam has a large earthquake-resistant margin. The failure processes of the cracked dam in strong earthquakes can be divided into two stages: the sliding stage and the overturning stage. The sliding stage ends near the peak acceleration, and the top block slides a long distance along the crack before the collapse occurs. The maximum sliding displacement of the top block will decrease with an increasing friction coefficient at the crack site.

Key words: seismic stability; concrete gravity dam; penetrated crack; plastic-damage model; hard contact algorithm; Coloumb friction model; joint opening

1 Introduction

Strong earthquakes may cause cracking of concrete gravity dams. Some cracks can penetrate through the monoliths, and the whole dam may break into several blocks. Recently, many researchers have focused on the case of penetrated cracks in seismic responses, because a dam is no longer a structure but rather becomes a system of blocks separated by penetrated cracks in such a case. Saini et al. (1972) first studied the rocking stability of the Koyna Dam with a penetrated crack by assuming that the dam had a penetrated crack at the elevation where the downstream slope changed abruptly. Harris et al. (2000) focused on the process of crack occurrence and propagation by shaking table tests. Malla and Wieland (2006) studied the

This work was supported by the National Basic Research Program of China (973 Program, Grant No. 2007CB714104), the National Natural Science Foundation of China (Grant No. 50779011), and the Innovative Project for Graduate Students of Jiangsu Province (Grant No. CX10B_202Z).

*Corresponding author (e-mail: syjiang@hhu.edu.cn)

Received Jan. 28, 2011; accepted Mar. 18, 2011

dynamic stability of detached concrete blocks in an arch dam. However, dealing with dynamic contact conditions at the crack site became a major challenge in these studies. The penalty approach was adopted in the incremental displacement constraint equation (IDCE) model (Zhu 2004) to simulate the contact condition at the crack site. Based on previous studies, Zhu and Pekau (2007) employed the finite element method (FEM) and the IDCE model to account for all the modes of motion along the cracks, and, in their studies, equivalent damping was introduced by considering its influence on the stability of a cracked concrete gravity dam. Pekau and Cui (2004) analyzed the two possible failure modes, overturning and sliding motions of the detached top block of a cracked dam using the distinct element method, and they revealed that the safety of the dam was ensured if the crack shape was horizontal or sloped upstream. Javanmardi et al. (2005) developed a theoretical model for considering transient water pressure variations along a seismic tensile concrete crack, and the model was introduced into an FEM program to analyze the seismic structural stability of concrete gravity dams. Ftima and Léger (2006) stated that gravity dams were likely to undergo cracking and sliding in the upper section during the action of strong earthquake ground motion and developed simplified computational procedures to generate professional recommendations and dam safety guidelines for the evaluation of the residual sliding displacement components of cracked concrete gravity dams. Wang (2008) studied two different types of detached blocks and analyzed their dynamic stability with the FEM procedure. All of these researchers stated that penetrated cracks may develop in dams during strong earthquake ground motion, and that dams with penetrated cracks can actually withstand subsequent earthquakes within a certain range. Thus, it is necessary to conduct the seismic stability analysis of concrete gravity dams with penetrated cracks.

In this paper, on the basis of the ABAQUS business software platform and using the Koyna Dam as a research subject, the placement of penetrated cracks was first determined using the concrete plastic-damage model based on the nonlinear FEM. Then, the hard contact algorithm and the Coloumb friction model were adopted to simulate the crack interaction both in the normal and tangential directions between detached concrete blocks. Finally, seismic stability analysis of a dam with two types of penetrated cracks was performed, and the analysis also covered the influence of the friction coefficient on the stability of the cracked dam.

2 Numerical models

The dam can be divided into several blocks by penetrated cracks, along which two surfaces are formed. When the two surfaces are in contact, they can transmit tangential forces, known as the friction force, as well as normal forces. The Coloumb friction model, which can simulate the crack interaction in the tangential direction, is often adopted in engineering analysis because of its brevity and applicability. The crack interaction in the normal direction can be simulated with the hard contact algorithm. Additionally, substantial energy dissipation

during earthquakes may occur, and can be represented by interior structural damping. In solving the contact problem, the contact region is unknown prior to the analysis, so the incremental methods are used to deal with the problem.

2.1 Description of hard contact algorithm

The hard contact algorithm can minimize the penetration between two contact bodies at the constraint location. When the two surfaces are in contact, any contact pressure can be transmitted between them. Once the two surfaces separate, the contact pressure immediately decreases to zero. Separated surfaces come into contact again when the clearance between them is reduced to zero.

2.2 Description of Coulomb friction model

The standard Coulomb friction model assumes that no relative motion occurs if the frictional stress τ_i is less than the critical stress τ_{crit} , which is proportional to the normal contact pressure p in the form $\tau_{\text{crit}} = \mu p$, where μ is the friction coefficient. The relationship between the elastic slip and interface shear stress τ_i satisfies Eq. (1):

$$\tau_i = k_s \gamma_i^{\text{el}} \quad (1)$$

where the subscript i means the coordinate direction i , and $i=1, 2$; γ_i^{el} is the elastic slip at the end of the current increment; and k_s is the stiffness of the elastic stick, and $k_s = \tau_{\text{crit}} / \gamma_{\text{crit}}$, where γ_{crit} is the allowable maximum elastic slip and is set to 0.5% of the average length of all contact elements in the model. For the elastic stick, the elastic slip γ_i^{el} is equal to the total slip γ_i . The incremental form of Eq. (1) can be expressed as

$$d\tau_i = k_s d\gamma_i + \frac{\tau_i}{\tau_{\text{crit}}} \mu dp \quad (2)$$

From Eq. (2), we can obtain the following formulation, which denotes the contact surface's tangential stiffness contribution to the whole system:

$$\begin{cases} \frac{d\tau_i}{d\gamma_i} = k_s \\ \frac{d\tau_i}{du_N} = \frac{\tau_i}{\tau_{\text{crit}}} \mu \frac{dp}{du_N} = \frac{\gamma_i}{\gamma_{\text{crit}}} \mu \frac{dp}{du_N} \end{cases} \quad (3)$$

where u_N is the overlap of the two surfaces.

When $\tau_i = \mu p$, relative motion between the two contact surfaces occurs. Assuming that the initial elastic slip at the current increment is $\bar{\gamma}_i^{\text{el}}$, and the plastic slip increment is $\Delta\gamma_i^{\text{sl}}$, the total slip increment $\Delta\gamma_i$ at the current increment can be expressed as

$$\Delta\gamma_i = \gamma_i^{\text{el}} - \bar{\gamma}_i^{\text{el}} + \Delta\gamma_i^{\text{sl}} \quad (4)$$

At the end of the current increment, the shear stress τ_i still follows Eq. (1). The relationship between the plastic slip increment $\Delta\gamma_i^{\text{sl}}$ and the interface shear stress τ_i is

$$\Delta\gamma_i^{\text{sl}} = \frac{\tau_i}{\tau_{\text{eq}}} \Delta\gamma_{\text{eq}}^{\text{sl}} \quad (5)$$

where $\Delta\gamma_{eq}^{sl}$ is the equivalent plastic slip increment. Substituting Eq. (1) and Eq. (5) into Eq. (4), the following equation can be obtained:

$$\tau_i = \frac{\bar{\gamma}_i^{el} + \Delta\gamma_i}{\gamma_{crit} + \Delta\gamma_{eq}^{sl}} \tau_{crit} \quad (6)$$

With $\gamma_i^{pr} = \bar{\gamma}_i^{el} + \Delta\gamma_i$, Eq. (6) can be simplified as follows:

$$\tau_i = \frac{\gamma_i^{pr}}{\gamma_{crit} + \Delta\gamma_{eq}^{sl}} \tau_{crit} \quad (7)$$

Substituting $\Delta\gamma_{eq}^{sl} = \gamma_{eq}^{pr} - \gamma_{crit}$, where $\gamma_{eq}^{pr} = \sqrt{\sum_{i=1}^2 (\gamma_i^{pr})^2}$, into Eq. (7), we can obtain

$$\tau_i = n_i \tau_{crit} \quad (8)$$

where $n_i = \gamma_i^{pr} / \gamma_{eq}^{pr}$. The incremental form of Eq. (8) is

$$d\tau_i = (\delta_{ij} - n_i n_j) \frac{\tau_{crit}}{\gamma_{eq}^{pr}} d\gamma_j + n_i \mu dp \quad (9)$$

where δ_{ij} is the Kronecker sign; and the subscript j means the coordinate direction j , where $j = 1, 2$. From Eq. (9), we can obtain the following formulas, which represent the contact surface's tangential stiffness contribution to the whole system:

$$\begin{cases} \frac{d\tau_i}{du_N} = n_i \mu \frac{dp}{du_N} \\ \frac{d\tau_i}{d\gamma_j} = 0 \end{cases} \quad (10)$$

2.3 Mechanism of energy dissipation

There are three ways to dissipate energy when a dam with penetrated cracks is subjected to a subsequent earthquake. The first way is through interior material friction, which is known as structural damping. The bottom block of the dam considered in this paper could be considered an independent structure with a fixed bottom. The first modal frequency of the bottom block was 2.64 Hz with a full reservoir, and the second modal frequency was 6.66 Hz. The equivalent viscous damping ratio ξ was set to 5%, the mass proportional damping α was 2.28, and the stiffness proportional damping β was 0.0009. The top block behaved nearly as a rigid body, and both the mass proportional damping α and the stiffness proportional damping β were set to zero. The second means to dissipate energy mainly involves friction along the crack, which can restrain relative motion between two contactors. This part of the dissipated energy could be accounted for by the Coloumb friction model mentioned above. The third energy dissipation mechanism takes place at the instant of contact, but the energy dissipated here should be very small, since only the elastic properties of concrete were considered and the plastic property was omitted in this study. Hence, this contribution could be conservatively set to zero.

2.4 Verification of numerical models

The numerical models mentioned above are verified in this section. Considering a free-standing block, shown in Fig. 1 (a), which is 1.02 m wide, and 4 m high, and has slenderness a of 0.25 rad, the motion modes possibly consist of slide, overturn, or slide-overturn depending on the level of ground acceleration $\ddot{u}_g(t)$, the width-height ratio b/h , and the friction coefficient μ . In Fig. 1(a), the block rotates clockwise when $\theta > 0$.

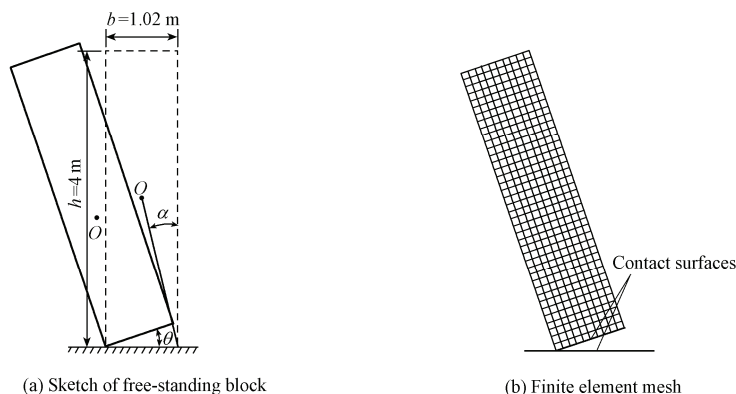


Fig. 1 Schematic diagram of free-standing block and finite element mesh

If the free-standing block is considered a rigid body, its rotation response under a one-sine pulse is given by Zhang and Makris (2001) with the ground acceleration:

$$\ddot{u}_g(t) = \begin{cases} a_p \sin(\omega_p t + \psi) & -\psi/\omega_p \leq t \leq (2\pi - \psi)/\omega_p \\ 0 & \text{otherwise} \end{cases} \quad (11)$$

where a_p is the amplitude of the acceleration, with $a_p = 6.32\alpha g$; g is the gravitational acceleration, with $g = 9.81 \text{ m/s}^2$; ω_p is the frequency of the one-sine pulse; and ψ is the initial phase angle, with $\psi = \sin^{-1}(\alpha g/a_p)$. To verify numerical models, the rigid body was assumed to be a deformable body and discretized into 10×40 mesh domains shown in Fig. 1(b). The bottom of the free-standing block was flat and had contact with the foundation along the base of the body. Applied loads included the weight of the block itself and the one-sine pulse. Considering the elastic impact, the coefficient of restitution of 1.0 was used in this study, which was slightly different from the value of 0.9 in Zhang and Makris (2001). Except for the coefficient of restitution, the parameters were identical with those in Zhang and Makris (2001). In addition, the friction coefficient is a major parameter in the numerical models and the mass density is also a necessary input. Although the analytical solution indicates that the rotation response of the block is independent of the friction coefficient and the mass density, the rotation response of the body is given with different friction coefficients (μ) of 0.8, 1.0, and 1.2 in Fig. 2(a), and different mass densities (ρ) of 100 kg/m^3 , 1000 kg/m^3 , and 2000 kg/m^3 in Fig. 2(b) based on the solution algorithm presented in the paper, and compared with the results of Zhang and Makris (2001).

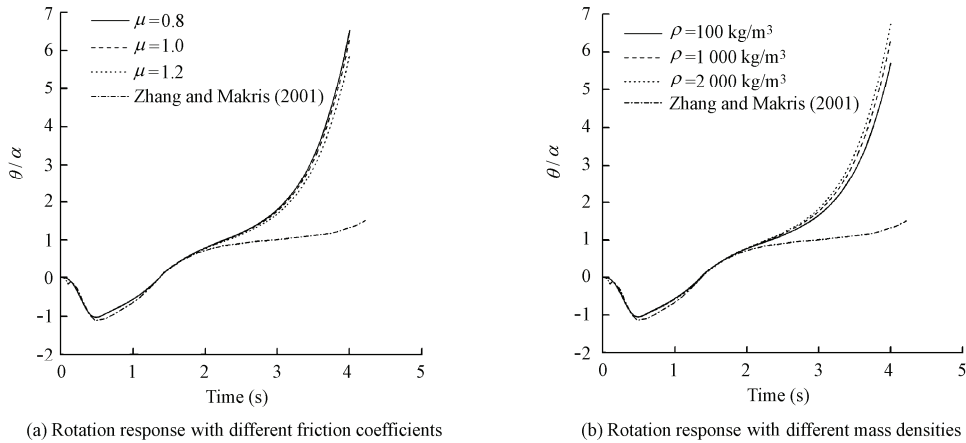


Fig. 2 Rotation responses of block

Both the numerical results and the literature's results show that the block may overturn after experiencing an impact when $a_p = 6.32\alpha g$. As shown in Fig. 2(a) and Fig. 2(b), the numerical results indicate that the rotation response of the block is independent of the friction coefficient and the mass density. Additionally, the form of the rotation history curve and its variation tendency obtained from numerical results are identical with those of Zhang and Makris (2001) before 2s. After 2s, due to the fact that the elastic impact is considered in the paper, the block overturns ahead of time. The overturning processes of the block are shown in Fig. 3. The rotation of the block reaches approximately 90° at 4s. Therefore, the validity of the numerical methods can be ensured, which can be used in subsequent case studies.

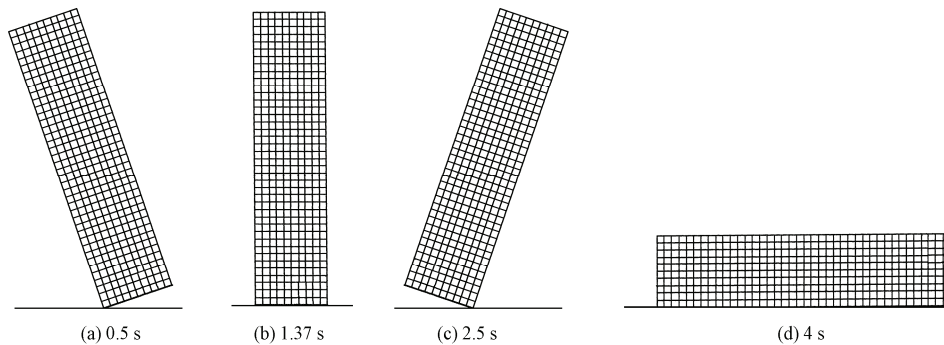


Fig. 3 Overturning processes of block

3 Determination of place of penetrated cracks

The Koyna Dam was subjected to a strong earthquake with a magnitude of 6.5 on December 11, 1967. The recorded ground accelerations of the earthquake had a peak value of 0.49g in the horizontal direction and 0.34g in the vertical direction, as plotted in Fig. 4.

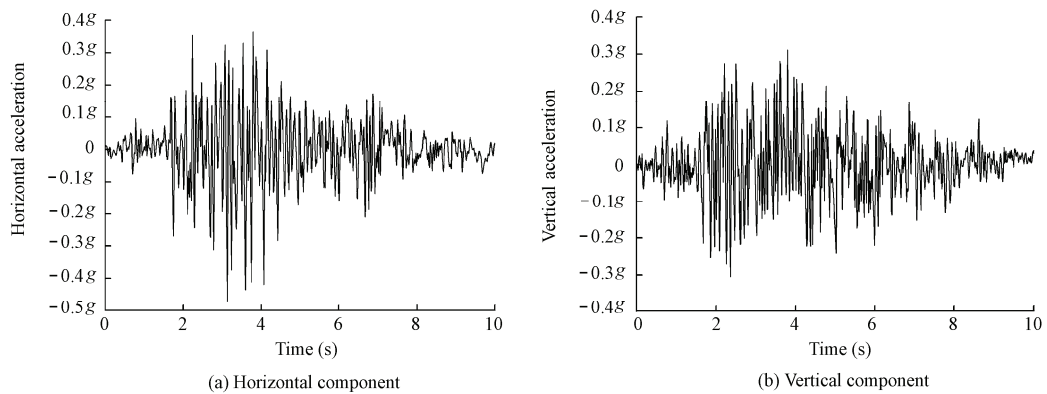


Fig. 4 Ground acceleration in Koyna earthquake on December 11, 1967

The cross-section of the dam shown in Fig. 5(a) is 103 m high and 14.8 m wide at the top, and 70 m wide at the bottom, with a sharp slope change on the downstream face at a height of 66.5 m. The discretized domain of the dam is shown in Fig. 5(b). The reservoir water level was 91.75 m at the time of the Koyna earthquake. The upstream wall of the dam was assumed to be straight and vertical, which was slightly different from the real configuration. The nonlinear FEM was employed, and the concrete plastic-damage model (Lubliner et al. 1989; Lee and Fenves 1998) was adopted to analyze the possible crack and damage modes of the dam. Assuming that the foundation was fully rigid, the boundary conditions were applied by constraining the degree of freedom of the nodes at the bottom face of the dam in the x and y directions. Applied loads included the weight of the dam for the first loading stage, the hydrostatic load for the second stage, and the hydrodynamic and seismic loads for the third stage. Hydrodynamic loads were calculated using the Westergaard added mass method (Westergaard 1933).

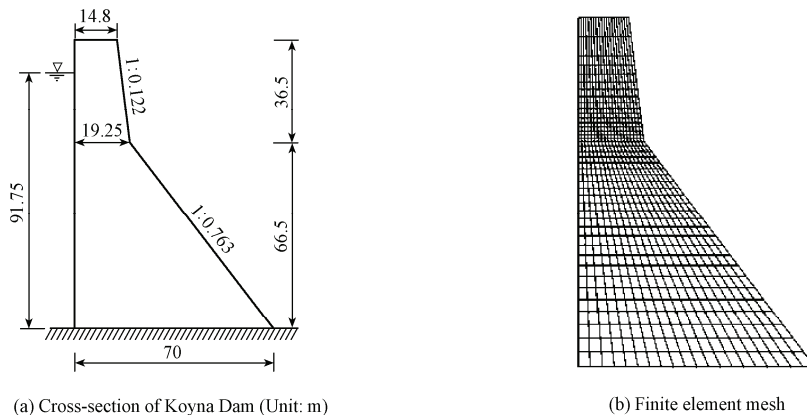
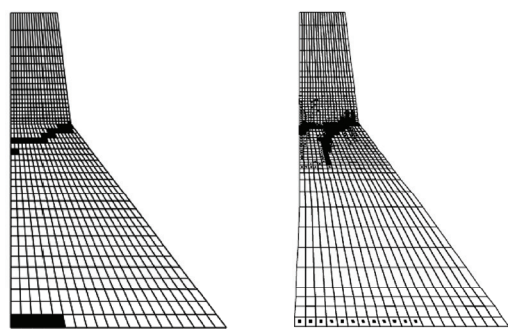


Fig. 5 Finite element model of Koyna Dam

The parameters of the Koyna Dam concrete material (Wang et al. 2000) are the elastic modulus E of 3.16×10^4 MPa, the Poisson ratio ν of 0.2, the density ρ of 2.64×10^3 kg/m³, the dilation angle ϕ of 36.31° , the compressive strength σ_{cu} of 24.60 MPa, and the tensile

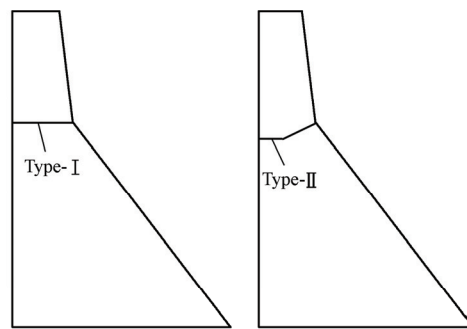
strength σ_{10} of 2.46 MPa.

Nonlinear analysis reveals two areas of damage (Fig. 6): (1) the upstream dam heel, and (2) the location where the downstream slope changes abruptly. The numerical results in this study (Fig. 6(a)) are identical with those of Wang et al. (2000) and Calayir and Karaton (2005), verifying the validity of the numerical result in this study. For comparison, Fig. 6(b) also shows the results from Calayir and Karaton (2005). Additionally, the concrete dam may be built in stages, which may lead to the formation of the weak interlayer interface. Therefore, two types of penetrated cracks may occur when the dam suffers from strong earthquakes (Fig. 7).



(a) Result of this study (b) Result of Calayir and Karaton (2005)

Fig. 6 Areas of dam damage



(a) Type-I crack (b) Type-II crack

Fig. 7 Two types of penetrated cracks

4 Stability analysis of detached top block

The dam is divided into two blocks by a penetrated crack from a previous strong earthquake. Without an external force, the dam will maintain its integrity because of the friction at the crack site, and the detached top block will be stable. However, the top block may slide, overturn, or even collapse during a subsequent strong earthquake. In addition, it is also possible that the seismic responses of the dam depend on the choice of numerical models and the parameters of the model. Due to the fact that the actual value of the model parameter is quite difficult to obtain, some related parameters may be studied, such as the friction coefficient, and their influences on the seismic responses are discussed in detail in Section 4.3. It should be mentioned that the assumption without distinguishing the static and dynamic friction coefficients is taken into consideration in most of the literature (Scalia and Sumbatyan 1996; Zhang and Makris 2001; Pekau and Cui 2004), and such an assumption is also used in this study. It should also be noted that a purely two-dimensional model can only be used to investigate the motion solely in the upstream or downstream direction, but, in reality, inter-monolith friction possibly exists.

4.1 Seismic response of cracked dam under 1967 Koyna earthquake

The stability of the Koyna Dam with a penetrated crack in the 1967 Koyna earthquake is assessed in this section. The blocks were assumed to be fully deformable and discretized into

quadrilateral elements. The hard contact algorithm and the Coulomb friction model mentioned above were used to simulate the normal and tangential behaviors of the crack. Since the detached top block can produce large sliding and overturning motions in strong earthquakes, it is necessary to consider the geometric nonlinearity and large deformation. The field shear test data for roller compacted concrete (RCC) at Dachaoshan Hydropower Station, which lies in the Basalt region, showed that the interlayer friction coefficient of RCC ranged from 0.96 to 1.48. The friction coefficient of the crack was set to 0.9 in this study, because the Koyna Dam was built with normal concrete, with the interlayer friction coefficient lower than that of RCC.

The stability of the dam was modeled using the Koyna earthquake on December 11, 1967 as an example. Two types of cracks, type I with a horizontal crack and type II with a curving crack (Fig. 7), are discussed in detail. The results show that the dam, with two types of cracks, respectively, remains stable when it is subjected to the 1967 Koyna earthquake conditions again. The movement histories of the top detached block with a type-I crack are shown in Fig. 8(a) and (b), and those with a type-II crack in Fig. 8(c) and (d).

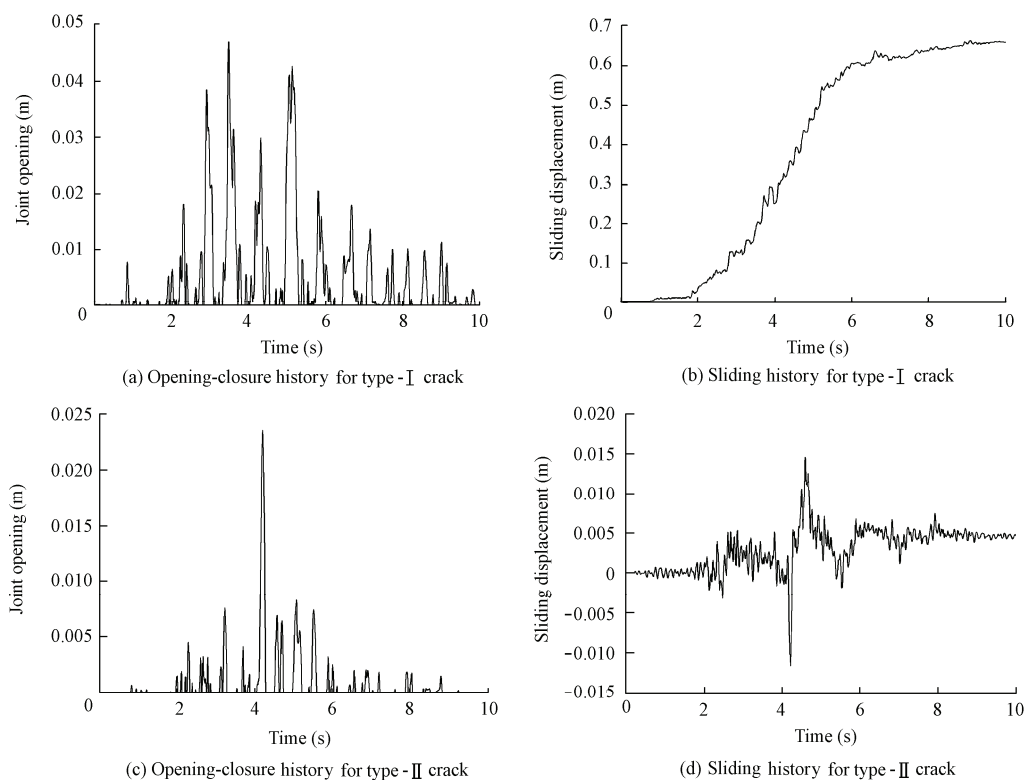


Fig. 8 Upstream movement histories of top detached block in 1967 Koyna earthquake

From Fig. 8, we can see that the sliding displacement of the top block with the type-I crack is dominant compared with the joint opening on the upstream surface, while the joint opening of the type-II crack is dominant because the curving crack increases the resistance against downstream sliding of the top block. The peak joint opening of the crack in type I on

the upstream surface occurs at 3.49 s, reaching 0.047 m, while in type II it occurs at 4.2 s, with the opening only 0.024 m. For the type-I crack, the sliding displacement tends to increase sharply near the peak earthquake acceleration (3.13 s) and to be stable after about 7s, which means that the top detached block can remain stable, and permanent sliding in the downstream direction reaches 0.66 m at the end of the earthquake. But for the type-II crack, the sliding curve is quite different, since the sliding displacement is no longer in the downstream direction consistently, but there occurs a reciprocating motion in a certain period. With the type-II crack, the corresponding sliding displacement of the top block is very small, and the permanent sliding is only 0.0046 m in the downstream direction at the end of the earthquake.

During the earthquake, the top block with a type-I crack consistently slides downstream, because the applied load effect on the upstream surface is larger than that on the downstream surface, i.e., both the hydrostatic and hydrodynamic loads are applied on the upstream surface. Because of a similar reason, the joint opening on the upstream surface is also dominant compared with that on the downstream surface. The profile of the type-I crack at a typical time with the peak opening occurring is shown in Fig. 9(a), in which the behaviors of the top block, i.e., the sliding of the top block and the joint opening, are displayed visually. But in the profile of the type-II crack, the difference is evident (Fig. 9(b)). Because the curving crack increases the resistance against downstream sliding of the top block, the top block may slide toward the upstream surface. From the discussion above, we can conclude that the curving crack is beneficial to the improvement of stability of the cracked dam.

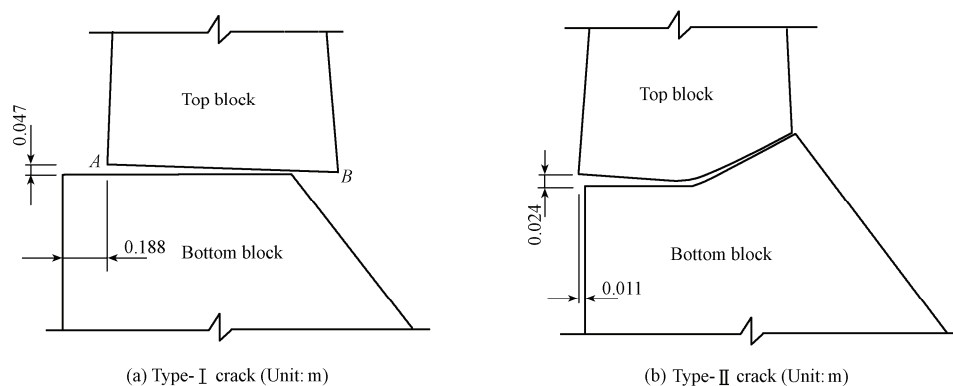


Fig. 9 Crack profile at typical time with peak opening

It can be seen from Fig. 9(a) that the top detached block can fully separate from the bottom block and float in the air. The mode of motion is usually called drifting motion. During the occurrence of drifting motion, the two lower corners *A* and *B* of the top block will simultaneously be away from the bottom block, whereas the vertical distances from the two corners to the top face of the bottom block and the joint openings on the upstream and downstream surfaces, respectively, are possibly unequal. To measure the intensity of drifting motion, the notion of drifting height is introduced. At the time of drifting motion, the joint

opening is defined as the drifting height, and the positive value denotes the drifting height on the upstream surface, while the negative value denotes the drifting height on the downstream surface. The drifting heights of two types of cracks are shown in Fig. 10. It can be seen that the drifting height on the upstream surface is dominant compared with that on the downstream surface, which means that the top detached block slides toward downstream more easily than upstream at the time of the drifting motion. The phenomena are especially reflected on the situation of the curving crack. However, the magnitude of the drifting height for the curving crack is quite smaller than that for the horizontal crack. It should also be observed that the peak joint opening for the horizontal crack quite possibly coupled with the drifting motion. It is still worth mentioning that due to the occurrence of the drifting motion, a great impact of the top block on the bottom block near the pivot point may lead to a localized crushing of concrete, but such research has not been involved in current works.

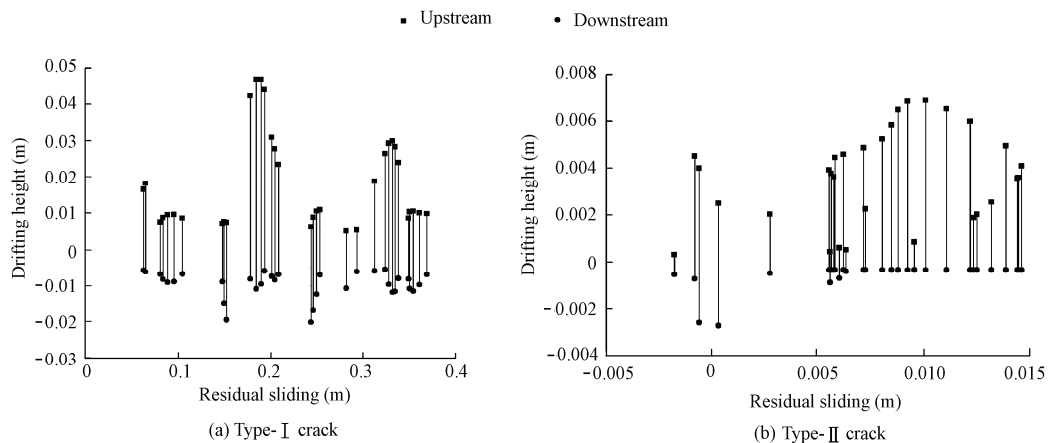


Fig. 10 Drifting height histories of two types of cracks

4.2 Earthquake-resistant margin of cracked dam

To study the seismic capacity of the dam with a penetrated crack, the stability is discussed in detail with several different peak ground accelerations. These accelerations were obtained by multiplying the horizontal and vertical components of that of the 1967 Koyna earthquake by factors of 2, 3, 4, and 5. The dam with a type-I crack will be unstable when the peak acceleration reaches five times the magnitude of the original Koyna earthquake. When the dam is unstable, the top block mainly slides downstream along the crack and the sliding displacement increases steadily until the collapse of the dam. The collapse processes of the dam with the type-I crack are shown in Fig. 11. For the cracked dam with a type-II crack, meanwhile, an earthquake of eight times the magnitude of the original Koyna earthquake can cause the failure of the dam, and the corresponding collapse processes are presented in Fig. 12. Both of the two types of cracked dams ultimately crush downstream.

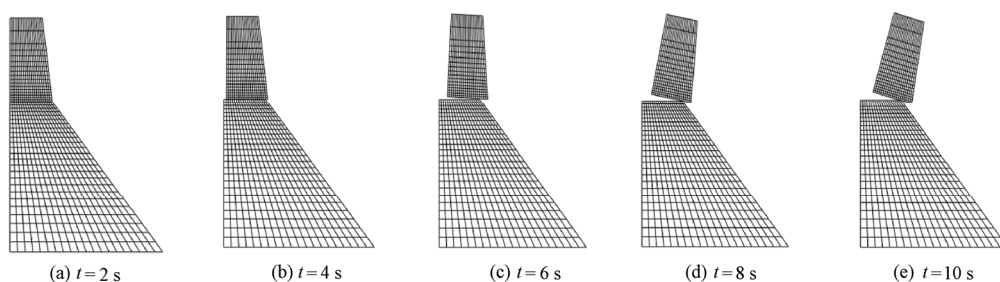


Fig. 11 Collapse processes of dam with type-I crack, with peak acceleration reaching five times the magnitude of original Koyna earthquake

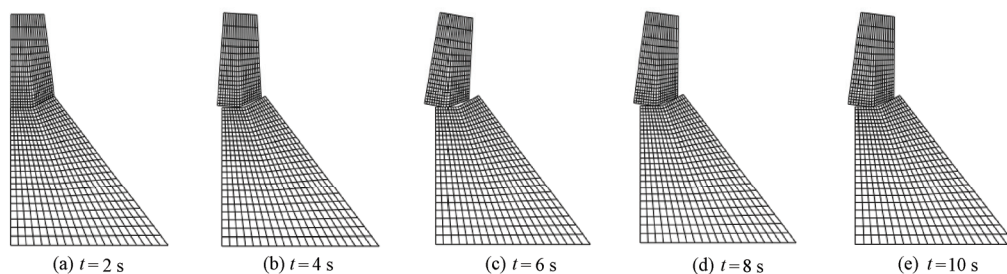


Fig. 12 Collapse processes of dam with type-II crack, with peak acceleration reaching eight times the magnitude of original Koyna earthquake

Fig. 13(a) and Fig. 13(b) show the upstream movement histories of the top block with the type-I crack with different peak accelerations, three times and five times the magnitude of the original Koyna earthquake. Fig. 13(c) and Fig. 13(d) show the upstream movement histories of the top block with the type-II crack, with the peak accelerations of five times, seven times, and eight times the magnitude of the original Koyna earthquake, respectively. When the dam is stable, the joint opening and the sliding curves tend toward the horizontal at the end of the earthquake. However, if the dam is unstable, the sliding curve increases steadily toward the end of the earthquake, indicating that the top block may collapse sometime, with the same being true of the opening curve.

With the analysis of the stability of the dam with a penetrated crack, we can see that the dam still has a large safety margin, since the dam with two types of cracks, respectively, will be unstable only when the peak ground acceleration reaches five times or eight times the magnitude of the original. The dam failure process can be divided into two stages: the sliding stage and the overturning stage. The sliding stage ends near the peak acceleration and the top block slides a long distance along the crack. Then, the sliding displacement abruptly increases, indicating that the dam is entering the overturning stage.

4.3 Seismic responses of cracked dam with different friction coefficients

In the analysis above, the friction coefficient μ is set to 0.9. For investigation of the relationship between the seismic responses and the friction coefficient at the crack site, the cracked dam with a type-I crack during the 1967 Koyna earthquake was taken as a research object, and the friction coefficient was experimentally varied, from 0.28 to 1.1. As shown in

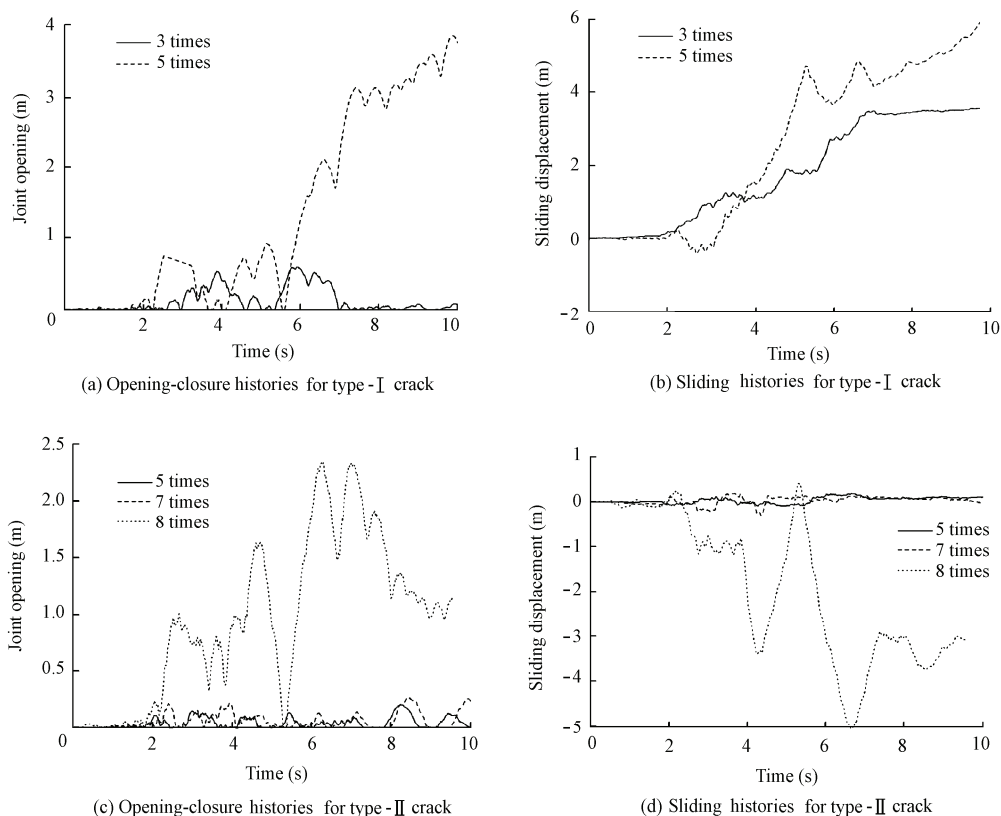


Fig. 13 Upstream movement histories of top detached block under different peak accelerations

Table 1, the peak sliding displacement of the top block decreases with the increase of the friction coefficient at the crack site when the dam remains stable. However, due to the severely nonlinear properties at the crack, the peak opening increases with the friction coefficient at the crack site only when the friction coefficient is less than 0.8. When the friction coefficient is greater than or equal to 0.8, the peak opening varies slightly. The dam will be unstable when the friction coefficient decreases to 0.28. Fig. 14 shows the sliding histories of the top block and the upstream opening and closure histories of the crack with different friction coefficients. With a lower friction coefficient, the permanent sliding of the top block obviously increases near the peak ground acceleration. From this discussion, one can see that the substantial sliding of the top block may induce dam instability when the friction coefficient is very low at the crack site.

Table 1 Peak sliding displacement and opening with different friction coefficients

μ	Peak sliding (m)	Peak opening (m)	μ	Peak sliding (m)	Peak opening (m)
1.1	0.562	0.054	0.7	1.457	0.165
1.0	0.441	0.048	0.5	1.569	0.077
0.9	0.658	0.047	0.4	2.379	0.073
0.8	0.711	0.047	0.3	4.688	0.050

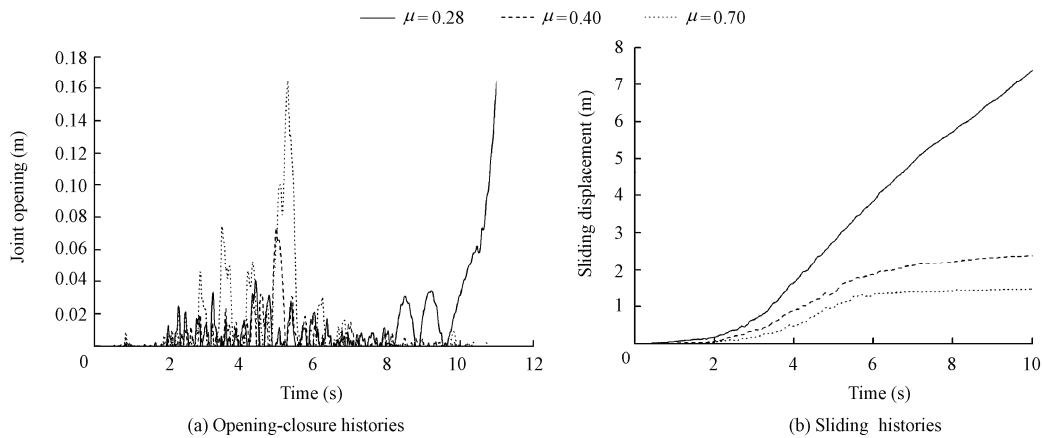


Fig. 14 Upstream movement histories of top detached block with different friction coefficients

5 Conclusions

Considering the geometric nonlinearity and large deformation at the crack site, the hard contact algorithm and the Coloumb friction model were used to simulate the collapse process of a dam with a penetrated crack. Some conclusions are drawn:

The earthquake resistance of a dam will decrease when the dam has a penetrated crack, but it still has a large safety margin. The dam with a straight horizontal crack will be unstable when the peak acceleration reaches five times the magnitude of the original Koyna earthquake, while the dam with a curving crack will be unstable with the peak acceleration of eight times the magnitude of the original Koyna earthquake. Thus, the shape of the crack has a significant effect on the earthquake-resistant margin of a cracked dam. To evaluate the safety of the cracked dam, the shape of the crack should be checked carefully.

When the top block is stable, the joint opening of the dam with a straight horizontal crack on the upstream surface is dominant compared with that on the downstream surface, and the primary motion mode to determine whether the dam is stable or not, is the tangential sliding. However, for the dam with a curving crack, the dominant motion mode is the joint opening-closure motion.

The stability of the dam can be improved with an increasing interlayer friction coefficient, since a higher friction coefficient can prevent the slide of the top block. The peak sliding displacement of the possible slide block decreases with the increase of the friction coefficient at the crack site. Due to severely nonlinear properties at the crack site, the peak joint opening increases with the crack friction coefficient only when the friction coefficient is less than 0.8. When the friction coefficient is greater than or equal to 0.8, the opening slightly varies.

References

Calayir, Y., and Karaton, M. 2005. Seismic fracture analysis of concrete gravity dams including dam-reservoir interaction. *Computers and Structures*, 83(19-20), 1595-1606. [doi:10.1016/j.compstruc.2005.02.003]

- Ftima, M. B., and Léger, P. 2006. Seismic stability of cracked concrete dams using rigid block models. *Computers and Structures*, 84(28), 1802-1814. [doi:10.1016/j.compstruc.2006.04.012]
- Harris, D. W., Snorteland, N., Dolen, T., and Travers, F. 2000. Shaking table 2-D models of a concrete gravity dam. *Earthquake Engineering and Structural Dynamics*, 29(6), 769-787. [doi:10.1002/(SICI)1096-9845(200006)29:6<769::AID-EQE925>3.0.CO;2-7]
- Javanmardi, F., Léger, P., and Tinawi, R. 2005. Seismic structural stability of concrete gravity dams considering transient uplift pressures in cracks. *Engineering Structures*, 27(4), 616-628. [doi:10.1016/j.engstruct.2004.12.005]
- Lee, J., and Fenves, G. L. 1998. Plastic-damage model for cyclic loading of concrete structures. *Journal of Engineering Mechanics*, 124(8), 892-900. [doi:10.1061/(ASCE)0733-9399(1998)124:8(892)]
- Lublinter, J., Oliver, J., Oller, S., and Oñate, E. 1989. A plastic-damage model for concrete. *International Journal of Solids and Structures*, 25(3), 299-326. [doi:10.1016/0020-7683(89)90050-4]
- Malla, S., and Wieland, M. 2006. Dynamic stability of detached concrete blocks in arch dam subjected to strong ground shaking. *Proceedings of First European Conference on Earthquake Engineering and Seismolog.* Geneva: European Association of Earthquake Engineering.
- Pekau, O. A., and Cui, Y. Z. 2004. Failure analysis of fractured dams during earthquakes by DEM. *Engineering Structures*, 26(10), 1483-1502. [doi:10.1016/j.engstruct.2004.05.019]
- Saini, S. S., Krishna, J., and Chandrasekaran, A. R. 1972. Behavior of Koyna Dam-Dec. 11, 1967 earthquake. *Journal of the Structural Division*, 98(7), 1395-1412.
- Scalia, A., and Sumbatyan, M. A. 1996. Slide rotation of rigid bodies subjected to a horizontal ground motion. *Earthquake Engineering and Structural Dynamics*, 25(10), 1139-1149. [doi:10.1002/(SICI)1096-9845(199610)25:10<1139::AID-EQE606>3.0.CO;2-S]
- Wang, G. L., Pekau, O. A., Zhang, C. H., and Wang, S. M. 2000. Seismic fracture analysis of concrete gravity dams based on nonlinear fracture mechanics. *Engineering Fracture Mechanics*, 65(1), 67-87. [doi:10.1016/S0013-7944(99)00104-6]
- Wang, H. B. 2008. Seismic stability of detached concrete block of concrete gravity dam. *Proceedings of the 14th World Conference on Earthquake Engineering.* Beijing: International Association for Earthquake Engineering.
- Westergaard, H. M. 1933. Water pressures on dams during earthquakes. *Transactions of the American Society of Civil Engineering*, 98(2), 418-433.
- Zhang, J., and Makris, N. 2001. Rocking response of free-standing blocks under cycloidal pulses. *Journal of Engineering Mechanics*, 127(5), 473-483. [doi:10.1061/(ASCE)0733-9399(2001)127:5(473)]
- Zhu, X. Y. 2004. *Seismic Behavior of Cracked Concrete Gravity Dams.* Ph. D. Dissertation. Montreal: Concordia University.
- Zhu, X. Y., and Pekau, O. A. 2007. Seismic behavior of concrete gravity dams with penetrated cracks and equivalent impact damping. *Engineering Structures*, 29(3), 336-345. [doi:10.1016/j.engstruct.2006.05.002]